EESD

by Jafril Tanjung

Earthquake Engineering & Structural Dynamics
The Journal of the International Association for Earthquake Engineering

EARTHQUAKE ENGINEERING & STRUCTURAL DYNAMICS
Earthquake Engng Struct. Dyn. 2016; **45**:999–1018
Published online 26 February 2016 in Wiley Online Library (wileyonlinelibrary.com). DOI: 10.1002/eqe.2715

Seismic response estimation method for earthquake-damaged RC buildings

Ho Choi[1], Yasushi Sanada[2,*,†], Hisatoshi Kashiwa[3], Yasuhiro Watanabe[4], Jafril Tanjung[5] and Huanjun Jiang[6]

[1]*Institute of Industrial Science, The University of Tokyo, Tokyo, Japan*
[2]*Graduate School of Engineering, Osaka University, Osaka, Japan*
[3]*Building Research Institute, Tsukuba, Ibaraki, Japan*
[4]*Graduate School of Engineering, Toyohashi University of Technology, Toyohashi, Aichi, Japan*
[5]*Engineering Faculty, Andalas University, Padang, Indonesia*
[6]*College of Civil Engineering, Tongji University, Shanghai, China*

SUMMARY

This study proposes a procedure for identifying spectral response curves for earthquake-damaged areas in developing countries without seismic records. An earthquake-damaged reinforced concrete building located in Padang, Indonesia was selected to illustrate the identification of the maximum seismic response during the 2009 West Sumatra earthquake. This paper summarizes the damage incurred by the building; the majority of the damage was observed in the third story in the span direction. The damage was quantitatively evaluated using the damage index *R* according to the Japanese guidelines for post-earthquake damage evaluation. The damage index was also applied to the proposed spectral response identification method. The seismic performance of the building was evaluated by a nonlinear static analysis. The analytical results reproduced a drift concentration in the third story. The *R*-index decreased with an increase in the story drift, which provided an estimation of the maximum response of the building during the earthquake. The estimation was verified via an earthquake response analysis of the building using ground acceleration data, which were simulated based on acceleration records of engineering bedrock that considered site amplification. The maximum response estimated by the *R*-index was consistent with the maximum response obtained from the earthquake response analysis. Therefore, the proposed method enables the construction of spectral response curves by integrating the identification results of the maximum responses in a number of earthquake-damaged buildings despite a lack of seismic records.

Received 19 June 2015; Revised 18 January 2016; Accepted 18 January 2016

KEY WORDS: damage index; earthquake response analysis; maximum response; nonlinear static analysis; reinforced concrete; spectral response curve

1. INTRODUCTION

Relative to developed countries, developing countries generally experience significant damage during earthquakes. The majority of earthquake disasters in developed countries provide valuable lessons for reducing future earthquake damage. The lessons learned from earthquakes in developing countries are hindered by limited resources. A lack of seismometer networks prevents a sufficient understanding of earthquake damage related to various factors, including ground motion characteristics, structural response characteristics, local structural materials and systems, and local construction skills. For the past several years, the authors have investigated earthquake-damaged buildings in Indonesia [1, 2].

*Correspondence to: Yasushi Sanada, Graduate School of Engineering, Osaka University, Osaka, Japan.
†E-mail: sanada@arch.eng.osaka-u.ac.jp

However, the earthquake damage to buildings could not be quantitatively related to the intensities of ground motions or structural responses because of the lack of seismic records. Therefore, this study proposes a method for identifying spectral response curves in earthquake-damaged areas without seismic records, referred to as the spectral response identification method. This paper provides and verifies a core procedure of the proposed method—namely, a procedure for identifying the maximum seismic responses of earthquake-damaged reinforced concrete (RC) buildings based on post-earthquake observation and nonlinear static analysis.

Figure 1 compares the spectral response identification method proposed in this study to the performance-based seismic design. The most recent performance-based seismic design utilizes building capacity spectra and earthquake demand spectra, as described in ATC (Applied Technology Council) -40 [3], FEMA (Federal Emergency Management Agency) -273 [4], ASCE (American Society of Civil Engineers) 41-06 [6], and the AIJ (Architectural Institute of Japan) guidelines [7]. These design codes provide the maximum responses of buildings under design spectra, as shown in Figure 1(a). In contrast, the proposed method regressively identifies a spectral response curve by integrating the maximum responses estimated for a number of buildings, as shown in Figure 1(b). To demonstrate the potential of the proposed method, the following investigations are conducted in this paper:

1. The damage to an earthquake-damaged RC building was quantitatively evaluated using a damage index;
2. The building performance was evaluated by a nonlinear static analysis;
3. The damage index for the building was quantitatively related to the maximum drift; and
4. The estimated maximum drift was verified via a comparison with a realistic earthquake response from a time-history analysis.

The European Macroseismic Scale [8], which addresses masonry and RC buildings, is used to evaluate earthquake damage to buildings. It defines a classification of damage grades by visual inspection but provides no damage index. This scale is not sufficient for the spectral response identification method proposed in this study, which requires a damage index (see 1) in the aforementioned investigation steps). Park and Ang [9] proposed a well-known damage index to

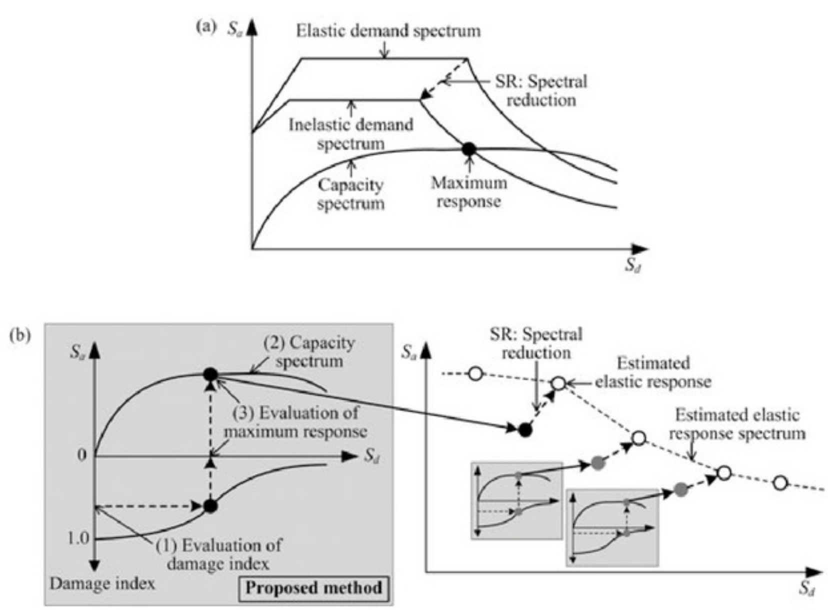

Figure 1. Concept of the spectral response identification method. (a) Schematic of performance-based seismic design. (b) Schematic of the spectral response curve identification.

DOI: 10.1002/eqe

quantitatively evaluate earthquake damage to RC buildings. However, the damage index cannot be obtained without the maximum response of each building component; thus, it cannot be applied to the proposed method, in which the maximum response is a resultant output (see 3). However, the Japan Building Disaster Prevention Association [10] provides another classification method (guideline), which has been practically applied after major earthquakes in Japan, such as the 1995 Kobe earthquake [11] and the 2011 Great East Japan earthquake [12]. The latest edition presented the damage index *R* for the quantitative evaluation of the residual seismic performance of earthquake-damaged RC buildings based on visual inspection. Therefore, the *R*-index was adopted for estimating the maximum responses of RC buildings in the proposed method, as described in this paper. The focus on RC buildings is reasonable for establishing the proposed method because RC buildings are widely used throughout the world, including developing countries.

The performance-based design, as shown in Figure 1(a), is realized by appropriate performance evaluations with sophisticated numerical analyses. These analyses commonly replace structural components by line elements with axial, flexure, and shear springs that represent nonlinear behavior [3]. Some micro-element models can consider axial-flexure interactions (e.g., [13]) and axial-flexure-shear interactions (e.g., [14]) based on the material properties of concrete and steel. However, in the case of analyses for RC moment-resisting frames that exhibit flexure-dominated behavior, the Takeda model [15] for macro-element models remains useful for simulating the structural behavior of RC members and was applied to the nonlinear static and earthquake response analyses performed in this study. Although many experimental studies have been conducted to evaluate the performance curves for RC members, limited studies evaluating unloading behavior have been reported (e.g., [16]). The unloading stiffness is a common interest in this study because it particularly affects the hysteretic behavior; thus, it was investigated based on an experimental database [17, 18].

2. OVERVIEW OF THE INVESTIGATED TYPICAL REINFORCED CONCRETE BUILDING IN INDONESIA

2.1. The 2009 West Sumatra, Indonesia earthquake

On 30 September 2009 at 5:16 pm local time, a magnitude 7.6 earthquake (USGS [19]) struck the southern coast of West Sumatra, Indonesia (0.72°S, 99.86°E, depth: 81 km) and caused moderate to heavy damage to the city of Padang, which is the capital of the province of West Sumatra. Many RC buildings were significantly damaged. However, seismic records for this earthquake were limited, as discussed in Chapter 4.

The authors conducted an earthquake damage investigation in Padang. During the investigation, a building of the Finance and Development Audit Agency (Badan Pengawasan Keuangan Dan Pebangunan (BPKP))—a five-story RC public office building constructed in 2003—was selected as a typical RC building in the surveyed area, and a damage class evaluation for each member was conducted according to the Japanese guidelines [10]. The basic concept of this guideline is briefly described in Section 2.3. In Indonesia, the present seismic design provisions for buildings were revised in 2002, mainly referring to the building codes of the USA and New Zealand based on the capacity design. The BPKP building was designed according to the present provisions.

2.2. Badan Pengawasan Keuangan Dan Pebangunan building

In this study, a BPKP building located in central Padang was selected to analytically estimate the seismic response during the earthquake. Figure 2 shows the BPKP building before and after the earthquake. Figure 3 shows the second-floor and third-floor plans with damage classes of RC columns that were evaluated according to the following method. The span length in the longitudinal (NS) and transverse (EW) directions was 6 m, as shown in Figure 3, and the story height was 3.5 m. Table I lists the structural details of the columns. The thickness of the slab was 120 mm. A nondestructive hammer test and rebar locating exercise were performed during the investigation because the structural drawings were not comprehensive. The results showed that the compressive strength of the concrete was 25.2 N/mm^2. A deformed bar of SD40 (nominal yield strength:

DOI: 10.1002/eqe

Figure 2. Views of the BPKP building before and after the earthquake. (a) Before the earthquake. (b) After the earthquake.

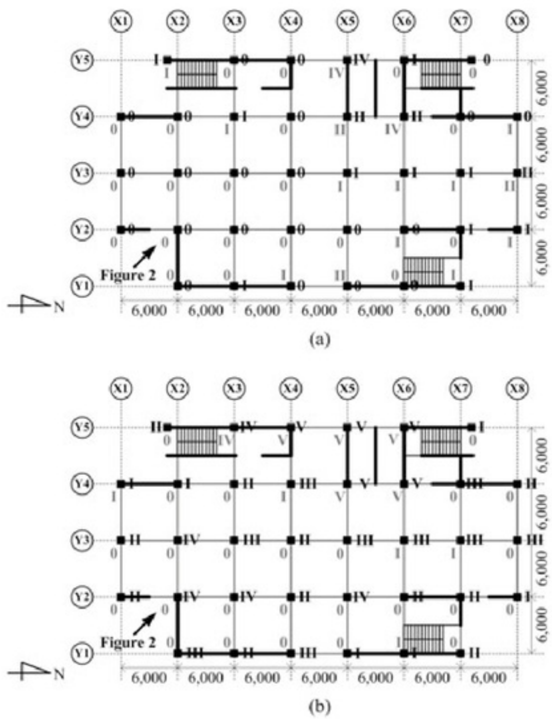

Figure 3. Floor plans and damage classes of the columns; the black and gray colors represent the damage classes (0 through V) in the longitudinal and transverse directions, respectively. (a) Second floor. (b) Third floor.

DOI: 10.1002/eqe

395 N/mm^2) and a round bar of SR24 (nominal yield strength: 235 N/mm^2) were employed for longitudinal reinforcements and shear reinforcements, respectively. Table II presents the mechanical properties of the concrete and reinforcements employed in the following analyses. All walls shown in Figure 3 were non-structural unreinforced masonry (URM) brick infill walls. The number of walls in the longitudinal direction exceeded the number of walls in the transverse direction. The damage overview of the BPKP building is summarized in the succeeding sections.

Damage of this building was mainly observed to vertical members such as columns and URM walls. On the other hand, damage to beams and beam column joints was not found. This building seemed to have good construction quality from the damage investigation. In the first story, damage to the main frames was minor; however, there was an open space between the Y2 and Y4 axes. The damage to the second story was more significant than the damage to the first story. Visible clear flexural cracks on the concrete surfaces were observed in the columns along the X5–Y4 and X6–Y4 axes (damage class II according to the Japanese guidelines [10], which are introduced in the succeeding sections), and significant concrete crush with exposed reinforcing bars was observed in the column along the X5–Y5 axis (damage class IV), as shown in Figure 3(a). The third story experienced the most significant damage in the transverse (EW) direction. As shown in Figure 3(b), damage to the west side of the building was substantial. Buckled and ruptured reinforcing bars were observed in the columns along the Y4 and Y5 axes (damage class V), and reinforcing bars were exposed in the columns along the Y2 and Y3 axes (damage class IV), as shown in Figures 3(b) and 4. In the fourth

Table I. Column details (unit: mm).

	1F & 2F	3F to 5F
Dimensions	550 × 550	450 × 450
Longitudinal reinforcement	16-#6	12-#6
Shear reinforcement	φ 9@150	φ 9@150

Table II. Mechanical properties of the concrete and reinforcements.

Compressive strength of the concrete	Yield stress of the longitudinal reinforcement	Yield stress of the shear reinforcement
25.2 N/mm^2	444 N/mm^{2*}	284 N/mm^{2*}

*The yield stresses of the longitudinal and shear reinforcements were estimated by considering an averaged over-stress of 49 N/mm^2.

(a) (b)

Figure 4. Significant damage to the third-story columns. (a) Damage class V (X5–Y4). (b) Damage class IV (X5–Y2).

DOI: 10.1002/eqe

and fifth stories, damage to the main frames was negligible: only flexural cracks were observed in some columns. Thus, this building exhibited a story failure mechanism in the transverse direction of the third story.

The authors carried out ambient vibration measurement using micro tremors for the BPKP building during the investigation. The fundamental periods in the longitudinal (NS) and transverse (EW) directions of the building were 0.69 s and 1.14 s, respectively.

2.3. *Residual seismic capacity ratio index R* [10]

The Japanese guidelines for a post-earthquake damage evaluation [10] provide a quantitative evaluation method for the residual seismic performance of earthquake-damaged buildings, where the performance is represented by the residual seismic capacity ratio index R given for each direction in each story. The R-index for each direction in each story of the investigated building was obtained as follows.

The R-index was calculated based on the damage to the columns, as noted earlier. First, damage classifications for all columns were performed according to Table III, in which the slender column damage is classified into six damage classes: 0 through V. The damage classes of I through IV correspond to flexural damage (refer to Figure 4(b)), while the damage class V approximately means shear failure after flexural yielding (refer to Figure 4(a)).

In the guidelines, the R-index was defined by Equation (1) with the seismic capacity reduction factor η listed in Table III. The R-index was evaluated considering the energy dissipation capacity ratio of an earthquake-damaged column to the original capacity, as illustrated in Figure 5.

$$R = \frac{\sum_{j=0}^{V} \eta_j \cdot n_j}{\sum_{j=0}^{V} n_j} \times 100\ (\%) \tag{1}$$

Table III. Damage class definition with the seismic capacity reduction factor η for slender reinforced concrete columns [10].

Damage class, j	Description of damage	η_j
0	No damage	1.0
I	Visible narrow cracks on the concrete surface (crack width is less than 0.2 mm)	0.95
II	Visible clear cracks on the concrete surface (crack width is 0.2–1.0 mm)	0.75
III	Local crush of cover concrete Significant wide cracks (crack width is 1.0–2.0 mm)	0.5
IV	Significant crush of concrete with reinforcing bar exposure Spalling of concrete cover (crack width exceeds 2.0 mm)	0.1
V	Buckling of the reinforcing bars Significant damage to the core concrete Visible vertical and/or lateral deformation of the column Visible settlement and/or leaning of the building	0

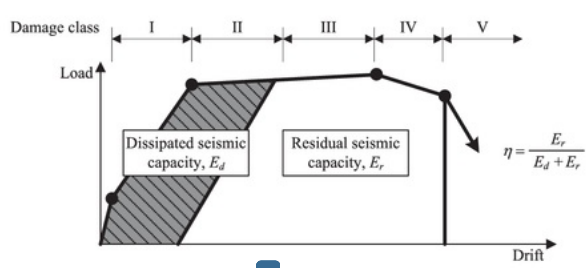

Figure 5. Definition of the seismic capacity reduction factor η.

DOI: 10.1002/eqe

where j is the damage class of the columns defined in Table III; η_j is the seismic capacity reduction factor for the columns with damage class j according to Table III; and n_j is the number of the columns with damage class j.

As a result, the R-indices of the BPKP building were evaluated, as shown in Table IV. The minimum value for the transverse direction in the third story was 54.1%, which was consistent with the observed damage.

3. SEISMIC RESPONSE ESTIMATION OF THE BPKP BUILDING

This chapter presents a method for estimating the maximum responses of earthquake-damaged buildings and applies it to the building investigated in the previous chapter. The experienced maximum drift of the BPKP building in the transverse direction—where the most significant damage was observed in the third story, as indicated in Table IV—was analytically estimated based on the residual seismic capacity ratio index R. Based on the estimated drift, the damage classes for all columns in the third story were also estimated and verified in comparison with the observed damage presented in Figure 3(b).

3.1. Nonlinear static analysis

3.1.1. Analytical assumptions. The structural damage of the BPKP building was mainly observed to the columns, as described in Section 2.2. Therefore, the nonlinear modeling of the columns is a key issue for the following analyses. The assumptions for nonlinear analyses are listed as follows. Figure 6 illustrates modeling for the structural components of the building.

1. The RC members were replaced by line elements with rigid zones at both ends; the length of each member was assumed to be $D/4$ (D is the depth of each member), as shown in Figure 6.

Table IV. R-indices for the Badan Pengawasan Keuangan Dan Pebangunan building.

Story	Longitudinal (NS) direction(%)	Transverse (EW) direction(%)
1	98.8	94.5
2	85.9	89.4
3	85.0	54.1
4	100.0	96.7
5	98.6	99.3

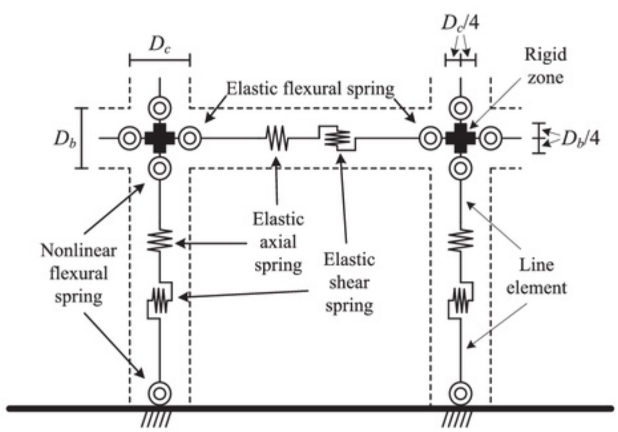

Figure 6. Modeling of the structural components.

Earthquake Engng Struct. Dyn. 2016; **45**:999–1018
DOI: 10.1002/eqe

2. The RC beams considered the elastic deformations because of minimal damage. However, the beam above/below the URM wall was assumed to be rigid considering the restriction of the beam deformation by the URM wall.
3. The RC columns considered nonlinear flexural characteristics and elastic axial and shear deformations. The Takeda model [15] was employed to represent nonlinear flexural behavior. The nonlinear performance curves were evaluated according to the stiffness degradation factor α_y in Subsection 3.1.2. The unloading stiffness was determined considering the degradation factor α of 0.4, which represents the unloading stiffness for the Takeda model, as described in Subsection 3.1.3.
4. Although the URM infill walls were considered with respect to the building weight, their strengths were disregarded because of the limited number of walls in the transverse direction for the analysis, as shown in Figure 3.
5. The foundations and slabs were regarded as rigid.
6. Dead loads and live loads—which were distributed to each node considering the tributary floor area—were estimated according to Indonesian guidelines [20].
7. The lateral force distribution for the static analysis was assumed to be an elastic first mode shape, as shown in Figure 7. The incremental pushover loads were applied toward the western direction in Figure 3 because the columns along the Y5 axis experienced the most severe damage in the transverse direction, which appeared to be caused by significant and varying compression due to predominant seismic loads in the western direction.

3.1.2. Evaluation of the column performance curves. In the following analyses, each column performance curve was replaced by a trilinear function with cracking and yielding points, as shown in Figure 8, based on Equations (2–6) for a practical design in Japan [21]. The cracking moment M_c and rotation θ_c were evaluated by Equations (2) and (3), respectively; and the yielding moment M_y and rotation θ_y were evaluated by Equations (4) and (5), respectively, based on common bending theories. However, in the case of the columns, varying axial forces were considered for N in Equation (4). The value of α_y given by Equation (6) provides a secant stiffness at the yielding point, as shown in Figure 8. The post-yield stiffness was assumed to be 0.1% of the elastic stiffness. These moments and rotations can be converted to corresponding shear forces and drifts by Equations (7–10).

$$M_c = 0.56\sqrt{f_c'}\cdot Z + \frac{ND}{6} \tag{2}$$

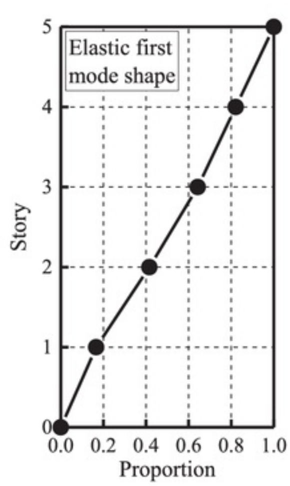

Figure 7. Lateral force distribution.

Earthquake Engng Struct. Dyn. 2016; **45**:999–1018
DOI: 10.1002/eqe

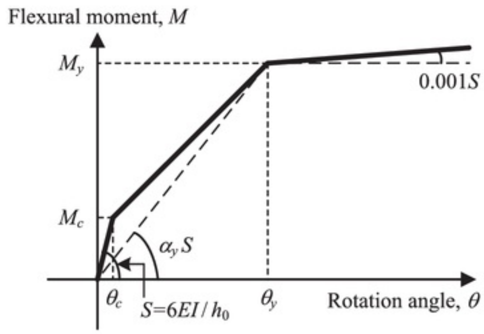

Figure 8. Performance curve of the column.

$$\theta_c = \frac{h_0}{6EI}\cdot M_c \tag{3}$$

$$M_y = 0.8\cdot a_t\cdot f_y\cdot D + 0.5\cdot N\cdot D\cdot\left(1 - \frac{N}{b\cdot D\cdot f_c'}\right) \tag{4}$$

$$\theta_y = \frac{h_0}{6EI}\cdot\frac{1}{\alpha_y}\cdot M_y \tag{5}$$

$$\alpha_y = (0.043 + 1.64\cdot n\cdot p_t + 0.043\cdot a/D + 0.33\cdot\eta_0)\cdot\left(\frac{d}{D}\right)^2 \tag{6}$$

$$Q_{Mc} = M_c(h_0/2) \tag{7}$$

$$Q_{My} = M_y(h_0/2) \tag{8}$$

$$\delta_c = \frac{h_0^3}{12EI}\cdot Q_{Mc} \tag{9}$$

$$\delta_y = \frac{h_0^3}{12EI}\cdot\frac{1}{\alpha_y}\cdot Q_{My} \tag{10}$$

where f_c' is the compressive strength of concrete; Z is the section modulus; N is the axial force; b, D, d, and h_0 are the width, depth, effective depth, and clear height, respectively; E is Young's modulus; I is the cross-sectional moment of inertia; a_t and p_t are the area of tensile reinforcements and the tensile reinforcement ratio, respectively; f_y is the yield stress of the longitudinal reinforcement; n is the ratio of the Young's modulus of the reinforcement to the Young's modulus of the concrete; a is the shear span; and η_0 is the axial force ratio ($=N/bDf_c'$).

3.1.3. Degradation factor for the unloading stiffness based on an experimental database. The degradation factor α for the unloading stiffness shown in Figure 9 was determined based on an experimental database [17]. In this study, the experimental results of three columns [17, 18] were selected because the structural characteristics were similar to the structural characteristics in the investigated building (see Table V for a comparison). The experimental results from the references

DOI: 10.1002/eqe

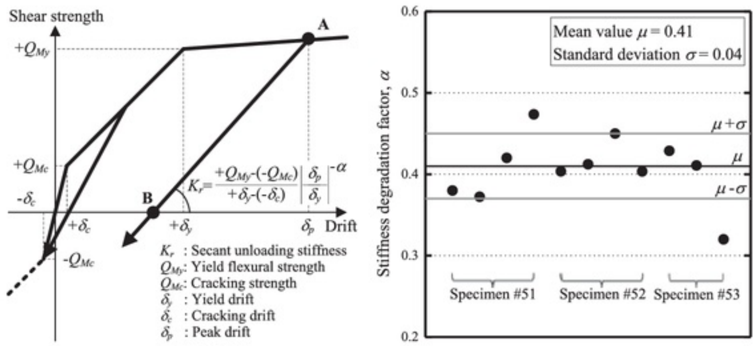

Figure 9. Post-yield secant unloading stiffness K_r for the Takeda model [15] and the stiffness degradation factor α from the test results of three specimens.

Table V. Comparison of the column characteristics.

		Width-to-depth ratio (b/D)	Shear span-to-depth ratio (a/D)	Tensile reinforcement-to-cross-sectional area ratio (%)	Axial load ratio (η_0)
BPKP building		1.0	3.9	0.57	0.12
Refs. [17], [18]	#51	1.0	3.0	0.61	0.12
	#52	1.0	3.0	0.61	0.11
	#53	1.0	3.0	0.61	0.11

BPKP, Badan Pengawasan Keuangan Dan Pebangunan.

are presented in Figure 10, and Figure 9 shows the values of factor α, which were regressively obtained from the post-yield secant unloading stiffness K_r between A and B in the figure [15]. The mean value μ and standard deviation σ were 0.41 and 0.04, respectively; therefore, a stiffness degradation factor α of 0.4 was employed in the following analyses.

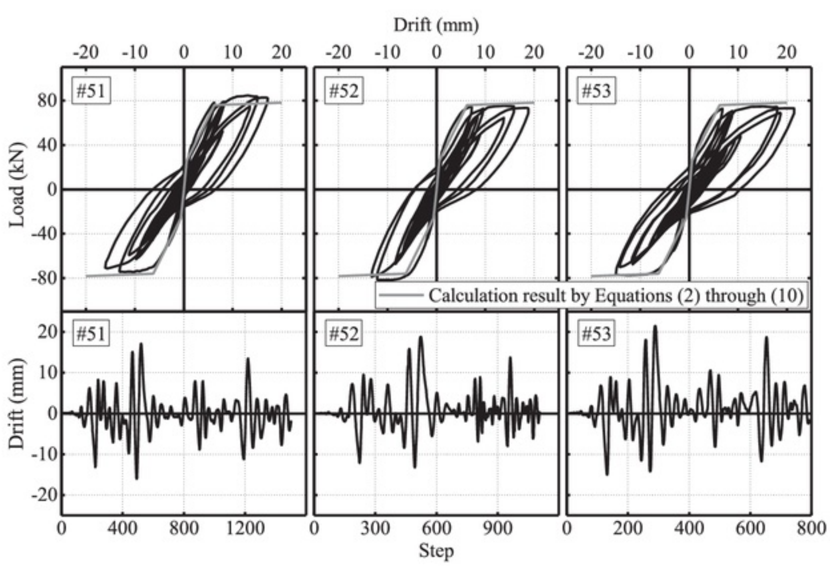

Figure 10. Load-drift relationships and drift time-histories of three specimens [17, 18].

3.1.4. Results of the nonlinear static analysis. Figure 8, based on Equations (2–10), is a key model for the column performance curve in this study. This modeling was verified in Figure 10, which compares the performance curves evaluated according to Figure 8 with the test results from the database. As a result, the analytical column performance curves were consistent with the test results.

Figure 11 shows the relationships between the story shear force and inter-story drift angle obtained from the nonlinear static analysis with the inter-story drift angle profiles along the building height. The inter-story drift angle in the third story was significantly larger than those on the remaining stories; this trend corresponded to the observed damage, as stated in the previous chapter.

3.2. *Maximum response estimation method based on the R-index*

3.2.1. Proposed procedure. The maximum response experienced by the BPKP building during the earthquake was estimated based on the *R*-index according to the following procedure:

1. The nonlinear static analysis of the BPKP building was performed under each incremental load step *j*, as noted in the previous section.
2. The index R_j at each step *j* was calculated for the transverse direction in the third story based on the damage classes of the third-story columns at the *j*th step, which were evaluated as described in the succeding paragraphs.
3. The experienced maximum responses of the third story and total building were estimated by finding the load step *j* to be $R_j = R_T$ (the target value of 54.1% in Table IV).

The damage classes that correspond to the load-drift relationships of the third-story columns were evaluated for this procedure 2. However, to simplify the procedure, the third-story columns were classified into three types with similar performance curves: exterior columns under varying tension along the Y1 axis, interior columns along the Y2–Y4 axes, and exterior columns under varying compression along the Y5 axis, considering the differences in the load-drift relationships under low, medium, and high axial loads, respectively, as illustrated in Figure 12 and Table VI. In Figure 12, the lateral strength at flexural cracking Q_{Mc} and yielding Q_{My} were evaluated by Equations (7) and (8), which provided the trilinear skeleton curve, as illustrated in Figure 8. On the other hand, the ultimate shear strength V_u [22] was evaluated by Equation (11), which can consider a decrease in the shear strength with an increase in the column plastic drift angle R_p (R_u–R_y shown in the following). Comparing Q_{My} and V_u, an ultimate drift angle R_u was obtained at the intersection between Q_{My} and V_u, as illustrated in Figure 13. The ultimate ductility ratio μ_u was evaluated as the ratio of R_u to R_y, where R_y was assumed to be a constant value of 0.67% [23], as shown in Table VI. However, the precise calculations from Equation (10) were approximately 0.67%. The damage class versus drift angle relationships for the three types of columns—which were determined based on the η index presented in Table III and Figure 5—are illustrated in Figure 12. Consequently, all the third-story columns were evaluated to show flexure-dominant behavior up to

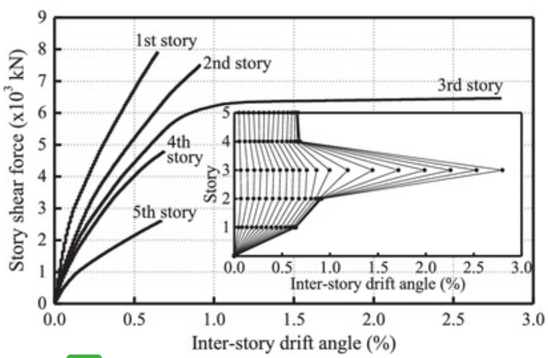

Figure 11. Story shear force – inter-story drift angle relationships and inter-story drift angle profiles along the building height.

DOI: 10.1002/eqe

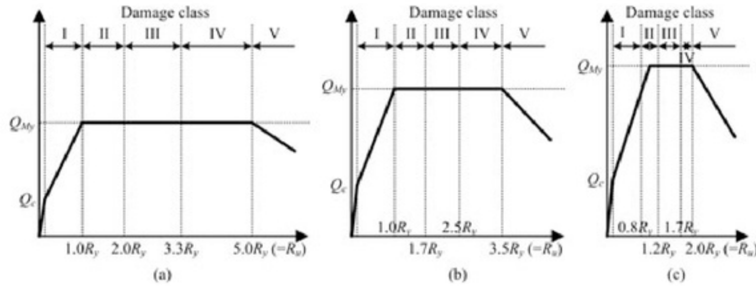

Figure 12. Damage class versus drift angle relationship models for the columns in the third story. (a) Y1 axis. (b) Y2–Y4 axes. (c) Y5 axis.

Table VI. Lateral strengths, drift angles, and ductility ratios of the columns in the third story.

	Strength at flexural yielding Q_{My} (kN) [23]	Ultimate shear strength V_u (kN) [22]	Yield drift angle R_y (%) [23]	Ultimate drift angle R_u (%) [22]	Ultimate ductility ratio μ_u (R_u/R_y)
Y1	134	242*	0.67	3.4	5.0
Y2 to Y4	184	242*	0.67	2.3	3.5
Y5	203	242*	0.67	1.4	2.0

* when $R_p = 0$

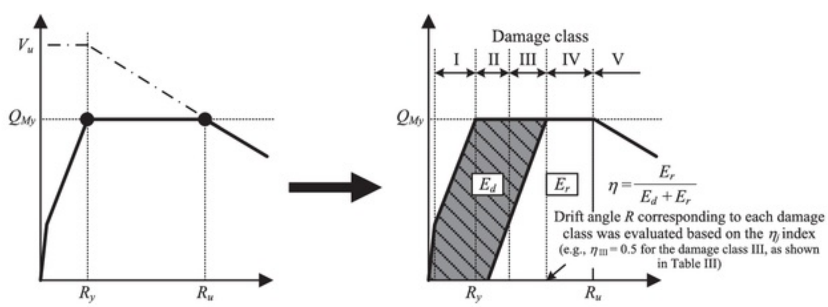

Figure 13. Evaluations of the ultimate drift angle R_u and damage class.

the damage class IV and shear failure beyond the damage class V. This failure mechanism was consistent with the observed mechanism, as mentioned in Section 2.3.

$$V_u = \mu \cdot p_{we} \cdot f_{wy} \cdot b_e \cdot j_e + \left(\nu \cdot f_c^{'} - \frac{5 \cdot p_{we} \cdot f_{wy}}{\lambda} \right) \cdot \frac{bD}{2} \cdot \tan\theta \quad (11)$$

where μ is the coefficient concerning the angle of concrete truss action (2-20R_p); R_p is an inelastic rotation of hinge region (rad); p_{we} is the shear reinforcement ratio in the hinge region ($a_w/(b_e\ s)$); a_w is the cross-sectional area of the shear reinforcements; b_e is the effective width of the column; s is the spacing between the shear reinforcements; f_{wy} is the yield stress of the shear reinforcement; j_e is the effective depth of the column; ν is the effectiveness factor for the concrete compressive strength in the hinge region ((1-20R_p)ν_0); ν_0 is the effectiveness factor for the concrete compressive strength outside the hinge region (0.7-$f_c^{'}$/200); λ is the effective area for the truss action (1-s/2j_e-b_s/4j_e); b_s is the largest distance between ties; and θ is the angle of the concrete arch strut.

DOI: 10.1002/eqe

3.2.2. Estimated maximum responses. Figure 14(a) shows the third-story performance curve in Figure 11 with the relationship between the *R*-index and inter-story drift angle in the third story. The third-story drift angle at the targeted *R*-index (54.1% in Table IV) was estimated to be 1.05%, and the corresponding story shear coefficient was approximately 0.295. The *R*-index decreased with an increase in the story drift, as shown in the figure. This tendency was caused by superimposing the relationships between the η index and story drift of all columns, which are illustrated in Figure 14(b) for the interior columns in the Y2–Y4 axes.

Figure 15 compares the damage classes of the third-story columns at the maximum inter-story drift angle of 1.05%, which was estimated by the proposed procedure with the observed damage classes in parentheses. The estimated damage classes were identical to the observations for more than 50% of the third-story columns. Although limited columns—such as X4–Y5—showed relatively large differences between the estimation and observation, the majority of the columns were similar with only one class gap.

Furthermore, the fundamental period of 1.12 s obtained based on the unloading stiffness from the estimated maximum response was consistent with that of 1.14 s by the ambient vibration measurement reported in Section 2.2.

4. SEISMIC RESPONSE ANALYSIS FOR VERIFICATION OF THE PROPOSED PROCEDURE

This chapter describes a time-history response analysis of the building using ground acceleration data, which were simulated based on acceleration records at engineering bedrock considering site amplification. The maximum responses estimated by the proposed procedure were compared with the maximum responses from the time-history analysis to verify the validity of the proposed procedure.

4.1. Estimation of the ground motion at the BPKP building site

Two seismographs were installed in the surrounding area of the BPKP building site prior to the 2009 West Sumatra earthquake. One seismograph was installed at Andalas University (UNAND), and the second seismograph was installed at a depth of 200 m at the Sinkarak Hydro Electric Power Plant (HEPP). Because Mangkoesoebroto reported that the seismograph at UNAND detected the occurrence of slippage because of an inadequate anchor to the foundation [24], the acceleration records from 200 m underground at the HEPP were employed in this study. The locations of the

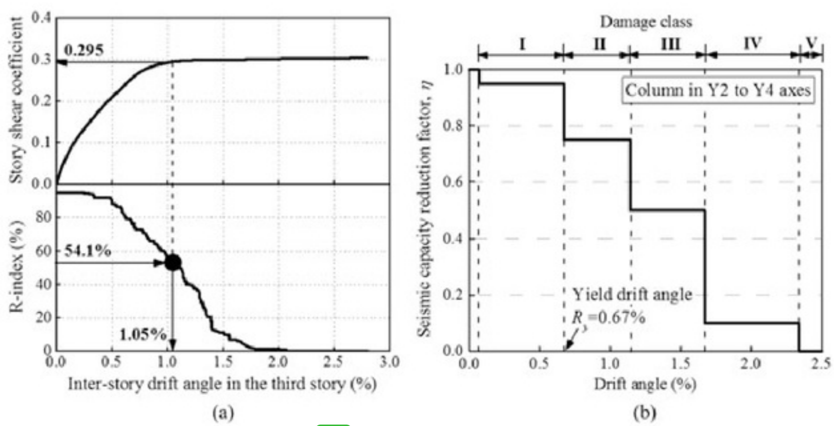

Figure 14. Maximum response estimated by the proposed procedure. (a) Performance curve for the third story and the *R*-index versus the inter-story drift angle relationship. (b) η versus the inter-story drift angle relationship for the columns in the Y2–Y4 axes.

DOI: 10.1002/eqe

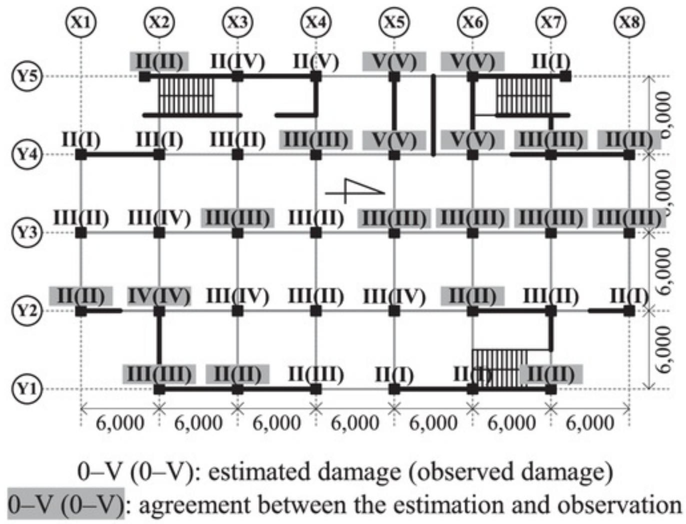

Figure 15. Estimated damage classes of the third-story columns at the maximum drift. 0–V (0–V): estimated damage (observed damage).

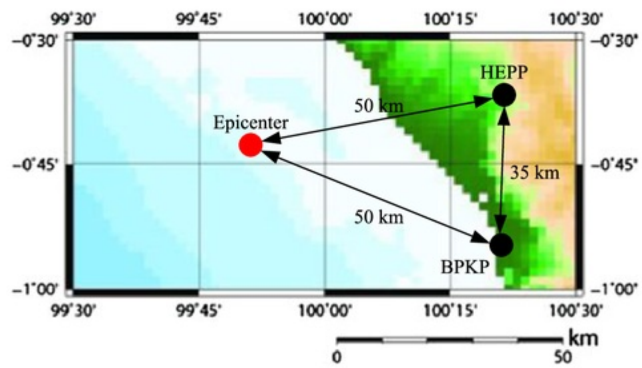

Figure 16. Locations of the Sinkarak Hydro Electric Power Plant (HEPP), Badan Pengawasan Keuangan Dan Pebangunan (BPKP) building, and epicenter.

HEPP, the BPKP building, and the epicenter are shown in Figure 16. The distances from the HEPP and BPKP building to the epicenter are approximately 50 km; however, the HEPP is located 35 km north of the building site.

The ground motion in the EW direction (the transverse direction of the building) at the building site during the earthquake was simulated based on the EW components of the seismic records at the HEPP (referred to as the HEPP bedrock records) to perform a time-history response analysis of the building. Figure 17 illustrates this simulation. Ground motion at the bedrock of the building site was assumed to be the incident wave (E) extracted from HEPP bedrock records. The acceleration data (2E) for the ground surface of the BPKP building (referred to as the BPKP GL simulation) were obtained by a seismic response analysis of the ground [25]. The surface soil of the BPKP building site was modeled based on references [26, 27]; however, the surface soil above a depth of 30 m was replaced based on the boring data from the BPKP building site. The shear wave velocity was calculated by Equation (12) and is shown in Table VII [28]. Table VIII and Figure 18 summarize the soil profiles.

DOI: 10.1002/eqe

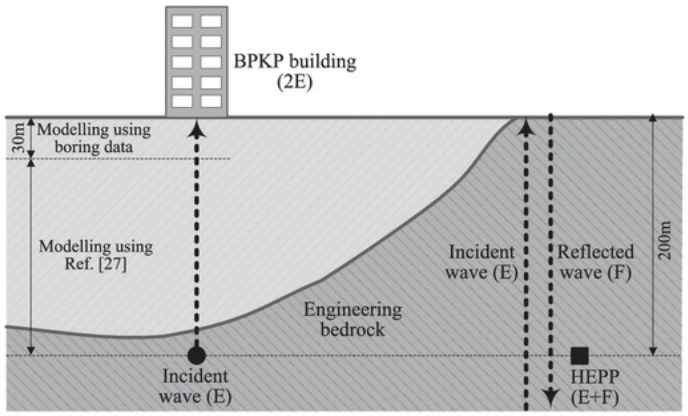

Figure 17. Concept of the ground motion simulation.

Table VII. Factors relating the soil type in Equation (12).

Soil type	Clay	Fine sand	Coarse sand
F_2	1.000	1.086	1.135

Table VIII. Ground model of the building site.

Depth (m)	N value	Soil type	Weight per unit volume (kN/m^3)	Shear wave velocity, V_s (m/s)
0–2	14	Fine sand	17	135
2–4	39	Fine sand	17	184
4–6	43	Fine sand	17	203
6–8	49	Fine sand	17	220
8–10	4	Clay	17	138
10–12	6	Clay	17	153
12–14	9	Clay	17	169
14–16	12	Clay	17	183
16–18	13	Clay	17	190
18–20	23	Clay	17	213
20–22	15	Clay	17	202
22–24	50	Coarse sand	17	287
24–26	54	Coarse sand	17	295
26–28	53	Coarse sand	17	299
28–30	58	Coarse sand	17	308
30–80	Unknown	Unknown	18	270
80–200	Unknown	Unknown	19	500

$$V_s = 68.79N^{0.171} \times H^{0.199} \times F_1 \times F_2 \tag{12}$$

where V_s is the shear wave velocity of each layer (m/s); N is the N-value of each layer; H is the depth of the bottom of each layer (m); F_1 is a factor for the geochronological classification of each layer (1.0); and F_2 is a factor for the soil type of each layer (Table VII).

Figure 19 illustrates the nonlinear dynamic soil properties for the time-history response analysis of the ground [29]. Figure 20 compares the acceleration time-histories between the HEPP bedrock records and BPKP GL simulation in the EW direction (the transverse direction of the building). The maximum

DOI: 10.1002/eqe

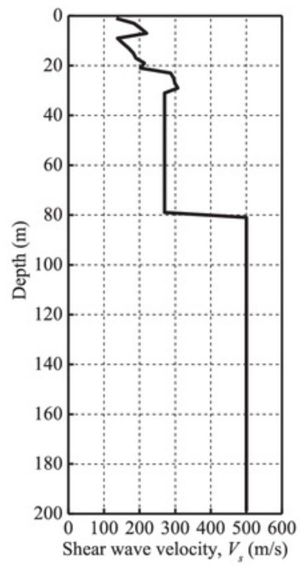

Figure 18. Shear wave velocity profile at the building site.

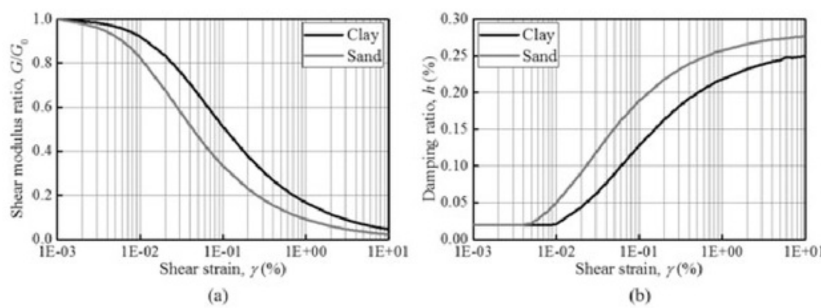

Figure 19. Nonlinear dynamic soil properties. (a) Shear modulus ratios. (b) Damping ratios.

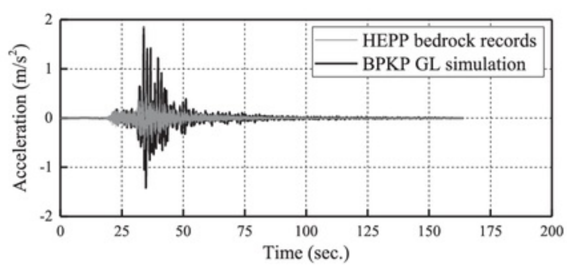

Figure 20. Acceleration time-histories of the Sinkarak Hydro Electric Power Plant (HEPP) bedrock records and BPKP GL simulation.

accelerations at the HEPP and BPKP were 0.94 and 1.85 m/s^2, respectively; thus, the amplification ratio was approximately twofold. The acceleration response spectra with 3% damping at both sites are compared in Figure 21. The predominant period at both sites was approximately 0.7 s; however, the spectrum of BPKP GL simulation exhibited large amplifications at 1.2 and 1.5 s.

DOI: 10.1002/eqe

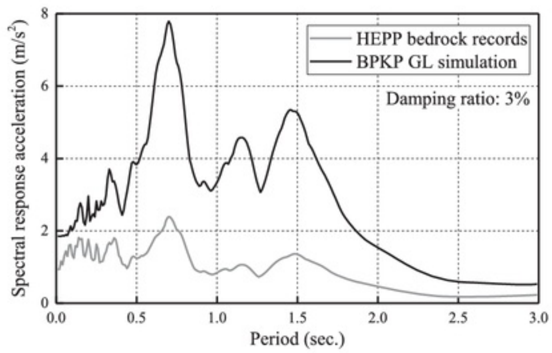

Figure 21. Acceleration response spectra of the Sinkarak Hydro Electric Power Plant (HEPP) bedrock records and BPKP GL simulation.

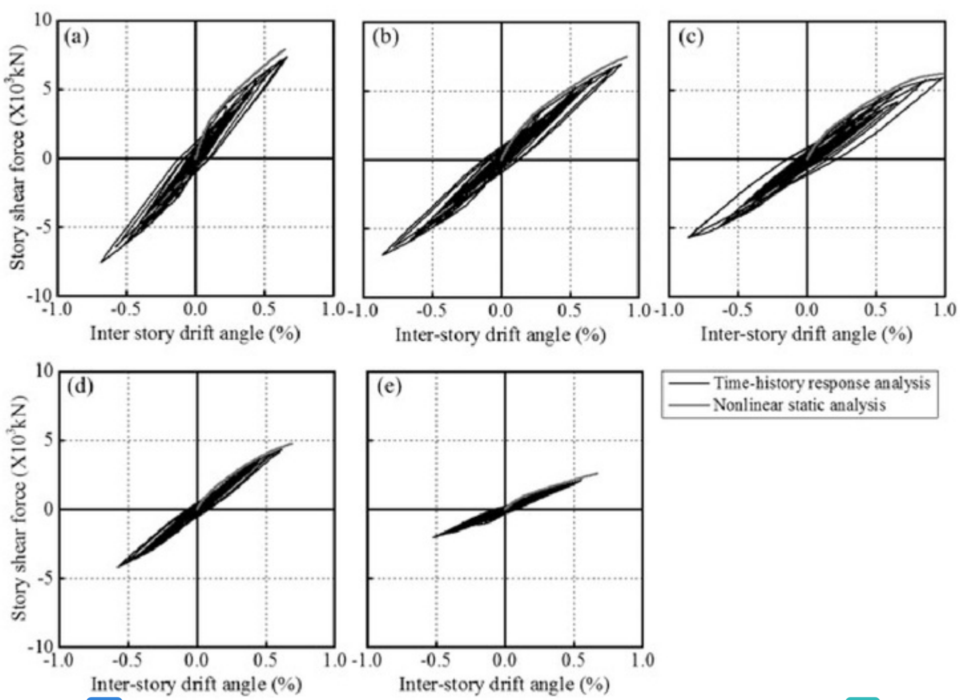

Figure 22. Relationship between the story shear force and inter-story drift angle of each story. (a) First story. (b) Second story. (c) Third story. (d) Fourth story. (e) Fifth story.

4.2. *Time-history response analysis of the BPKP building under the BPKP GL simulation*

The time-history response analysis of the BPKP building was performed in the transverse (EW) direction of the BPKP GL simulation obtained per the previous section. The analytical model of the building was identical to the analytical model in the nonlinear static analysis, which was previously discussed; however, tangent stiffness proportional damping with a damping coefficient of 3% was assumed. The damping value was an approximate average of observed damping coefficients (2.3%

DOI: 10.1002/eqe

to 3.6%) obtained by random decrement (RD) technique [30] using the ambient vibration measurement data described in Section 2.2.

Figure 22 shows the relationship between the story shear force and inter-story drift angle of each story, and Figure 23 compares the profile of the maximum inter-story drift angles from the time-history analysis with the profile from the proposed procedure. The profiles of the maximum inter-story drift angles from the proposed procedure are consistent with profiles from the time-history analysis. Therefore, the maximum response estimation method that was proposed in the previous chapter provided a reliable estimation of the seismic intensity of the earthquake-damaged area without seismic records.

4.3. *Prospective procedure for the spectral response identification*

A spectral response point for the BPKP building was estimated by the spectral response identification method proposed in this study, as shown in Figure 24. However, the response point was regarded as the elastic response because the estimated maximum response occurred approximately at the yield point, as shown in Figures 14 and 22. Thus, an elastic response spectrum can be regressively identified by integrating the maximum responses estimated for a number of buildings based on the proposed procedure, as shown in Figure 24. To complete the proposed method, additional studies are needed to verify that conventional methods and/or equations (e.g., 3) for converting inelastic responses to elastic responses can be carefully applied to targeted buildings considering local

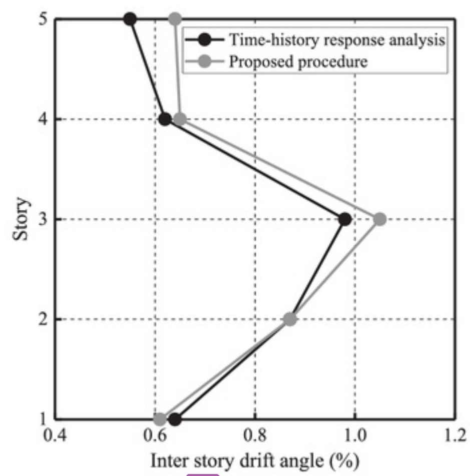

Figure 23. Comparison between the maximum inter-story drift profiles from the proposed method and the time-history analysis.

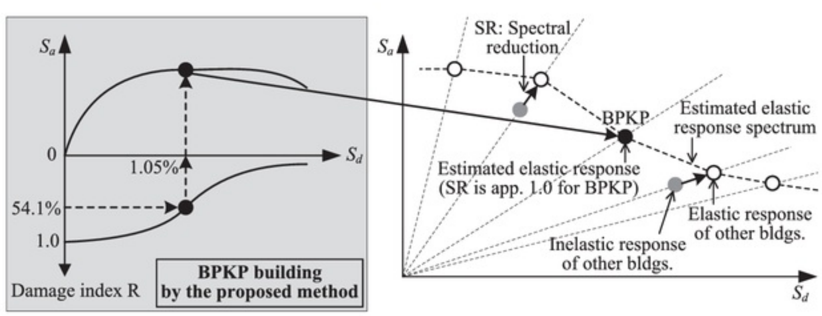

Figure 24. Schematic of the proposed spectral response identification procedure.

DOI: 10.1002/eqe

characteristics, such as structural materials, systems, and construction skills. In this paper, the proposed procedure was applied to the building to form the weak story collapse (column-sway) mechanism. In future studies, the procedure will be applied to well-designed buildings to form a beam-yielding total collapse mechanism and/or buildings with irregular configuration according to the same logic applied in this paper.

5. CONCLUSIONS

This study proposed a spectral response identification method to estimate the seismic intensity of an earthquake-damaged area without seismic records. This paper presented and verified the core procedure of the proposed method to estimate the maximum responses of earthquake-damaged RC buildings based on post-earthquake damage observation and nonlinear static analysis. The major findings are summarized as follows:

1. The post-earthquake damage evaluation of the BPKP building, which was damaged by the 2009 West Sumatra earthquake in Indonesia, provided the lowest residual seismic capacity (R-index) for the transverse direction in the third story, which was consistent with the actual damage observed in the building.
2. The nonlinear static analysis of the building in the transverse direction adequately simulated the inter-story drift concentration in the third story. The R-index, which was analytically evaluated for the building, decreased with an increase in the inter-story drift in the third story, which indicated the feasibility of estimating the maximum responses of the building based on this index.
3. The procedure for estimating the maximum responses of earthquake-damaged buildings based on the R-index was proposed and applied to the BPKP building. Consequently, the maximum inter-story drift for the third story was estimated to be 1.05%. In addition, the damage classes of the third-story columns at the drift corresponded with the observed damage.
4. The ground motion at the building site was simulated based on the acceleration records of engineering bedrock considering site amplification that were applied to the time-history response analysis of the building. Thus, the maximum inter-story drift profile from the time-history analysis was nearly identical to the profile that was estimated by the procedure proposed in this paper. Therefore, the proposed method will contribute to the estimation of seismic intensity of earthquake-damaged areas without seismic records.

REFERENCES

1. Sanada Y, Kishimoto I, Kuroki M, Sakashita M, Choi H, Tani M, Hosono Y, Fauzan, Musalamah S, Farida F. Preliminary report on damage to buildings due to the September 2 and 30, 2009 earthquakes in Indonesia. *Proceedings of the Eleventh Taiwan-Korea-Japan Joint Seminar on Earthquake Engineering for Building Structures*, Kyoto, Japan, 2009; 297–306.
2. Choi H, Sanada Y, Kuroki M, Sakashita M, Tani M, Hosono Y, Musalamah S, Farida F. Comparing damage to building structures due to the 2009 West Java earthquake in Indonesia. *The 2nd International Conference on Earthquake Engineering and Disaster Mitigation*, Surabaya, Indonesia, 2011; E-9–E-18.
3. Applied Technology Council (ATC). *Seismic evaluation and retrofit of concrete buildings. Volume 1*. ATC-40, Report No. SSC, 1996; 96–01.
4. Applied Technology Council (ATC). NEHRP guidelines for the seismic rehabilitation of buildings. Report No. FEMA 273 (ATC-33 Project), 1997.
5. American Society of Civil Engineers (ASCE). Prestandard and commentary for the seismic rehabilitation of buildings. Report No. FEMA 356, 2000.
6. American Society of Civil Engineers (ASCE). Seismic rehabilitation of existing buildings. ASCE 41–06, 2007.
7. Kabeyasawa T. An outline of AIJ guidelines for performance evaluation of earthquake resistant reinforced concrete buildings. *Proceedings of the International Workshop on Performance-Based Seismic Design Concepts and Implementation*, Bled, Slovenia, 2004; 27–38.
8. Grunthal G. European macroseismic scale 1998. *Cahiers du Centre Europeen de Geodynamique et de Seismologie* 1998; **15**:1–99.
9. Park YJ, Ang A. Mechanistic seismic damage model for reinforced concrete. *Journal of Structural Engineering* 1985; **111**(4):722–739. DOI:10.1061/(ASCE)0733-9445(1985)111:4(722).

10. Nakano Y, Maeda M, Kuramoto H, Murakami M. Guideline for post-earthquake damage evaluation and rehabilitation of RC buildings in Japan. *13th World Conference on Earthquake Engineering*, Vancouver, B.C., Canada, 2004; Paper No. 124.
11. Architectural Institute of Japan (AIJ). Preliminary reconnaissance report of the 1995 Hyogoken-Nanbu earthquake. Tokyo, Japan, **1995**.
12. Architectural Institute of Japan (AIJ). *Preliminary Reconnaissance Report of the 2011 Tohoku-Chiho Taiheiyo-Oki Earthquake*. Springer: Tokyo, Japan, 2012.
13. Li K, Aoyama H, Otani S. Reinforced concrete columns under varying axial load and bi-directional lateral load reversals. *Proceedings of Ninth Conference on Earthquake Engineering*, Tokyo-Kyoto, Japan, 1988; VIII537–VIII542.
14. Kim Y, Kabeyasawa T, Matsumori T, Kabeyasawa T. Numerical study of a full-scale six-story reinforced concrete wall-frame structure tested at E-defense. *Earthquake Engineering & Structural Dynamics* 2012; **41**:1217–1239. DOI:10.1002/eqe.1179.
15. Takeda T, Sozen MA, Nielsen NM. Reinforced concrete response to simulated earthquakes. *Journal of Structural Division, ASCE* 1970; **96**(ST12):2557–2573.
16. Erberik MA, Kurtman B. A detailed evaluation on degrading behavior of structural systems. *Proceedings of the 9th U.S. National and 10th Canadian Conference on Earthquake Engineering*, Toronto, Ontario, Canada, 2010; Paper No. 369.
17. Pacific Earthquake Engineering Research Center. PEER structural performance database (SPD). <http://nisee.berkeley.edu/spd/>. (Oct. 20, 2012)
18. Kanda M, Shirai N, Adachi H, Sato T. An analytical study on elasto-plastic hysteretic behaviors of R/C members (in Japanese). *Proceedings of the Japan Concrete Institute (JCI)* 1988; **10**(3):313–318.
19. USGS Website. <http://escweb.wr.usgs.gov/share/mooney/134.pdf>
20. SNI-03-1727-1989-F. <http://ja.scribd.com/doc/160254997/SNI-03-1727-1989-F-1#scribd>
21. Kabeyasawa T, Shoihara H, Otani S, Aoyama H. Analysis of the full-scale seven-story reinforced concrete test structure. *Journal of the Faculty of Engineering, The University of Tokyo* 1983; **37**(2):432–478.
22. Ichinose T. A shear design equation for ductile R/C members. *Earthquake Engineering & Structural Dynamics* 1992; **21**(3):197–214. DOI:10.1002/eqe.4290210302.
23. Japan Building Disaster Prevention Association (JBDPA), Standard and technical manual for seismic evaluation of existing reinforced concrete buildings, 2001.
24. Mangkoesoebroto SP. Padang earthquake of September 30, 2009. Why it is so devastating. Seminar dan Pameran Haki Perkembangan dan Kemajuan Konstruksi Indonesia, 2010. <https://wiryanto.files.wordpress.com/2010/08/16-sindur-p-mangkoesoebroto-paper.pdf>
25. Yoshida N. A computer program for DYNamic response analysis of level ground by EQuivalent linear method (DYNEQ). Version 3.25 (September, 2004), Revised from Original version (May, 1995).
26. Ono Y, Kiyono J, Rusnardi PR, Noguchi T. Microtermor observation in Padang City, Indonesia to estimate site amplification of seismic ground motion. Proceeding of International Symposium on a Robust and Resilient Society against Natural Hazards and Environmental Disasters and the Third AUN/SEED-Net Regional Conference on Geodisaster Mitigation 2010; **386–391**.
27. Noguchi T, Ono Y, Kiyono J, Horio T, Kubo M, Ikeda T, Putra RR. Determination of the subsurface structure of Padang City, Indonesia using microtremor exploration (in Japanese). *Journal of Japan Society of Civil Engineers (JSCE), Division A* 2010; **66**(1):30–39.
28. Ohta Y, Goto N. Empirical shear wave velocity equations in terms of characteristic soil indexes. *Earthquake Engineering & Structural Dynamics* 1978; **6**(2):167–187. DOI:10.1002/eqe.4290060205.
29. Otani S, Hiraishi H, Midorikawa M, Teshigawara M. New seismic design provisions in Japan, *The 2000 Fall ACI Annual Convention*, Toronto, Canada, 2000.
30. Tamura Y, Suganuma S. Evaluation of amplitude-dependent damping and natural frequency of buildings during strong winds. *Journal of Wind Engineering and Industrial Aerodynamics* 1996; **59**(2–3):115–130.

EESD

ORIGINALITY REPORT

23%	%	23%	3%
SIMILARITY INDEX	INTERNET SOURCES	PUBLICATIONS	STUDENT PAPERS

PRIMARY SOURCES

1	Maidiawati, Yasushi Sanada. "R/C frame-infill interaction model and its application to Indonesian buildings", Earthquake Engineering & Structural Dynamics, 2017 Publication	3%
2	Tomomi Suzuki, Ho Choi, Yasushi Sanada, Yoshiaki Nakano, Kazuto Matsukawa, Devjyoti Paul, Polat Gülkan, Baris Binici. "Experimental evaluation of the in-plane behaviour of masonry wall infilled RC frames", Bulletin of Earthquake Engineering, 2017 Publication	2%
3	Fajfar, Peter, and Michael Fardis. "Announcement by the Publisher : Announcement by the Publisher", Earthquake Engineering & Structural Dynamics, 2016. Publication	2%
4	Yuebing Li, Yasushi Sanada. "Seismic strengthening of existing RC beam-column joints by wing walls", Earthquake Engineering & Structural Dynamics, 2017	2%

Publication

5	"Issue Information", Earthquake Engineering & Structural Dynamics, 2016. Publication	2%
6	Yasushi Sanada, Rokhyun Yoon, Takumi Akahori, Yuto Ojio, Ho Choi, Yousok Kim. "Softening effects of RC nonstructural flat walls on ductile concrete buildings", Earthquake Engineering & Structural Dynamics, 2017 Publication	1%
7	Sanada, Yasushi. "Investigation and Analysis of Buildings Damaged during the September 2007 Sumatra, Indonesia Earthquakes", Journal of Asian Architecture and Building Engineering, 2008. Publication	1%
8	Maeda, Masaki, and Dae Eon Kang. "Post-Earthquake Damage Evaluation of Reinforced Concrete Buildings", Journal of Advanced Concrete Technology, 2009. Publication	1%
9	"High Tech Concrete: Where Technology and Engineering Meet", Springer Nature, 2018 Publication	1%
10	Advances in Structural Engineering, 2015. Publication	1%

11	Lee, Kang Seok, and Sung Woo Shin. "A New Methodology for Performance-based Seismic Evaluation of Low-rise Reinforced Concrete Buildings Using Nonlinear Required Strengths", Journal of Advanced Concrete Technology, 2013. Publication	<1%
12	Li, Yuebing, Yasushi Sanada, Susumu Takahashi, Koki Maekawa, Ho Choi, and Kazuto Matsukawa. "Seismic Performance Evaluation and Strengthening of RC Frames with Substandard Beam-Column Joint: Lessons Learned from the 2013 Bohol Earthquake", Journal of Earthquake and Tsunami, 2016. Publication	<1%
13	Lombardi, D., and S. Bhattacharya. "Evaluation of seismic performance of pile-supported models in liquefiable soils : Seismic Performance of Pile-Supported Models in Liquefiable Soils", Earthquake Engineering & Structural Dynamics, 2016. Publication	<1%
14	Shakeri, Kazem, and Samaneh Ghorbani. "A pushover procedure for seismic assessment of buildings with bi-axial eccentricity under bi-directional seismic excitation", Soil Dynamics and Earthquake Engineering, 2015. Publication	<1%

15	Khoo, Hsen-Han, Keh-Chyuan Tsai, Ching-Yi Tsai, Cheng-Yu Tsai, and Kung-Juin Wang. "Bidirectional substructure pseudo-dynamic tests and analysis of a full-scale two-story buckling-restrained braced frame : Bidirectional Pseudo-Dynamic Tests and Analysis of a Two-Story BRB Frame", Earthquake Engineering & Structural Dynamics, 2016. Publication	<1%
16	Vafaei, Mohammadreza, Azlan bin Adnan, and Ahmad Baharuddin Abd. Rahman. "Real-time Seismic Damage Detection of Concrete Shear Walls Using Artificial Neural Networks", Journal of Earthquake Engineering, 2013. Publication	<1%
17	Kim, S.P.. "An alternative pushover analysis procedure to estimate seismic displacement demands", Engineering Structures, 200812 Publication	<1%
18	Sanada, Yasushi, Yoshiaki Nitta, Takuya Tomonaga, and Yuta Sashima. "Experimental Study on Performance Evaluation of an Indonesian R/C Building Damaged by the 2009 Sumatra Earthquake", Applied Mechanics and Materials, 2011. Publication	<1%
19	T. Ichinose. "A shear design equation for ductile	

R/C members", Earthquake Engineering & Structural Dynamics, 1992
Publication <1%

20 Masato Saitoh. "Chapter 6 Application of a Highly Reduced One- Dimensional Spring-Dashpot System to Inelastic SSI Systems Subjected to Earthquake Ground Motions", InTech, 2012
Publication <1%

21 Shirai, Kazutaka, and Norio Inoue. "A Seismic Response Estimation Method for RC Structures using Random Vibration Theory", Journal of Advanced Concrete Technology, 2014.
Publication <1%

22 Kazuto Matsukawa, Masaki Maeda. "Methodology to evaluate the collapse limit state of R/C frames based on the seismic response spectrum", Japan Architectural Review, 2018
Publication <1%

23 Xiang, Ping, Akira Nishitani, Shohei Marutani, Kenzo Kodera, Tomohiko Hatada, Ryuta Katamura, Kiyoshi Kanekawa, and Takashi Tanii. "Identification of yield drift deformations and evaluation of the degree of damage through the direct sensing of drift <1%

displacements : Yield Deformation and Damage Evaluation through Displacement Sensing", Earthquake Engineering & Structural Dynamics, 2016.
Publication

24 A. Benavent-Climent, S. Mota-Páez. "Earthquake retrofitting of R/C frames with soft first story using hysteretic dampers: Energy-based design method and evaluation", Engineering Structures, 2017
Publication
<1 %

25 Junxian Zhao, Ruobing Chen, Zhan Wang, Yi Pan. "Sliding corner gusset connections for improved buckling-restrained braced steel frame seismic performance: Subassemblage tests", Engineering Structures, 2018
Publication
<1 %

26 Barbara Wohlfarth, Marie-José Gaillard, Wilfred Haeberli, Kerry Kelts. "Environment and climate in southwestern Switzerland during the last termination, 15-10 ka BP", Quaternary Science Reviews, 1994
Publication
<1 %

27 Maidiawati, , Yasushi Sanada, Daisuke Konishi, and Jafril Tanjung. "Seismic Performance of Nonstructural Brick Walls Used in Indonesian R/C Buildings", Journal of Asian Architecture
<1 %

and Building Engineering, 2011.
Publication

---

28 Mamoru Iwata. "A Damage-Controlled Structure Using Buckling-Restrained Knee Braces", Structural Engineering International, 11/01/2011 <1%
Publication

---

29 Martín-Pérez, B., and S. J. Pantazopoulou. "Mechanics of Concrete Participation in Cyclic Shear Resistance of RC", Journal of Structural Engineering, 1998. <1%
Publication

---

30 Rokhyun Yoon, Yasushi Sanada, Takumi Akahori. "Seismic Performance Evaluation of RC Moment-Resisting Frames with Typical Non-Structural Walls in Japan", Journal of Advanced Concrete Technology, 2017 <1%
Publication

---

31 Takeuchi, Toru, Ryota Matsui, and Saki Mihara. "Out-of-plane stability assessment of buckling-restrained braces including connections with chevron configuration : Stability Assessment of BRBs with Chevron Configuration", Earthquake Engineering & Structural Dynamics, 2016. <1%
Publication

---

32 Lu, Y.. "An analytical model for dynamic

response of beam-column frames to impulsive ground excitations", International Journal of Solids and Structures, 200702

Publication

<1%

33 Shakeri, K.. "A story shear-based adaptive pushover procedure for estimating seismic demands of buildings", Engineering Structures, 201001

Publication

<1%

34 Peng, Y., Z. Mei, and J. Li. "Stochastic seismic response analysis and reliability assessment of passively damped structures", Journal of Vibration and Control, 2013.

Publication

<1%

35 Chung-Che Chou. "Column restraint in post-tensioned self-centering moment frames", Earthquake Engineering & Structural Dynamics, 2009

Publication

<1%

36 Aydemir, Cem, and Mustafa Zorbozan. "Uncertainty Analysis of Flexural Overstrength Ratio for RC Columns", Journal of Structural Engineering, 2012.

Publication

<1%

37 Suita, Keiichiro, Yuko Shimada, Motohide Tada, Yuichi Matsuoka, Satoshi Yamada, and Kazuhiko Kasai. "Full scale shaking table

<1%

collapse experiment on 4-story steel moment frame : Part 2 detail of collapse behavior", Behaviour of Steel Structures in Seismic Areas STESSA 2009, 2009.
Publication

38	Lee, Kang Seok, Ho Choi, Sang Whan Han, and Sung-Bok Lee. "A Practical Rapid Screening Method for Evaluating the Seismic Capacity of Low-rise Reinforced Concrete Buildings", Journal of Advanced Concrete Technology, 2011. Publication	<1%
39	Springer Series in Geomechanics and Geoengineering, 2014. Publication	<1%
40	Submitted to Christchurch Polytechnic Institute of Technology Student Paper	<1%
41	S. M. Wilkinson. "Observations of damage to buildings from M w 7.6 Padang earthquake of 30 September 2009", Natural Hazards, 05/05/2012 Publication	<1%
42	Farrow, K.T.. "SDOF displacement ductility demands based on smooth ground motion response spectra", Engineering Structures, 200410	<1%

Publication

43	Huanjun Jiang, Bo Fu, Xilin Lu, Linzhi Chen. "Seismic Damage Assessment of RC Members by a Modified Park-Ang Model", Advances in Structural Engineering, 2016 Publication	<1%
44	Alıcı, F. S., and Halûk Sucuoğlu. "Prediction of input energy spectrum: attenuation models and velocity spectrum scaling : Input Energy Spectrum", Earthquake Engineering & Structural Dynamics, 2016. Publication	<1%
45	Ellingwood, Bruce R., Berk Taftali, and Reginald DesRoches. "Seismic Performance Assessment of Steel Frames with Shape Memory Alloy Connections, Part II – Probabilistic Seismic Demand Assessment", Journal of Earthquake Engineering, 2010. Publication	<1%
46	Yasushi Sanada, Yuebing Li, Koki Maekawa. "Experimental Verification of Seismic Strengthening by Wing Wall Installation for RC Buildings with Substandard Beam-column Joints", Procedia Engineering, 2017 Publication	<1%
47	Nakamura, N.. "Seismic response analysis of deeply embedded nuclear reactor buildings	<1%

considering frequency-dependent soil impedance in time domain", Nuclear Engineering and Design, 200807
Publication

48	Chen, Hung-Ming, and Wei-Ko Kao. "Computer-Aided Model Generation for Nonlinear Structural Analysis Using a Structural Component Model Database", Journal of Computing in Civil Engineering, 2008. Publication	<1%
49	Bai, Yongtao, and Guoliang Bai. "Pseudo-Dynamic and Quasi-Static Testing of an Irregular Steel Concrete Composite Frame with Wing Walls", International Journal of Structural Stability and Dynamics, 2014. Publication	<1%
50	Geotechnical Geological and Earthquake Engineering, 2015. Publication	<1%
51	Costa, Alexandre A., Andrea Penna, and Guido Magenes. "Seismic Performance of Autoclaved Aerated Concrete (AAC) Masonry: From Experimental Testing of the In-Plane Capacity of Walls to Building Response Simulation", Journal of Earthquake Engineering, 2011. Publication	<1%

52 Wu, Bin, Yongsheng Chen, Guoshan Xu, Zhu Mei, Tianlin Pan, and Cong Zeng. "Hybrid simulation of steel frame structures with sectional model updating : Hybrid Simulation of Frame Structures with Sectional Model Updating", Earthquake Engineering & Structural Dynamics, 2016.
Publication <1%

53 Liu, Kuang-Yen, Witarto Witarto, and Kuo-Chun Chang. "Composed analytical models for seismic assessment of reinforced concrete bridge columns : COMPOSED ANALYTICAL MOODELS FOR RC BRIDGE COLUMNS", Earthquake Engineering & Structural Dynamics, 2014.
Publication <1%

54 Kim, Kil-Hee, Woo-Bum Kim, Jin-Man Kim, and Sang-Woo Kim. "Composite Strut and Tie Model for Reinforced Concrete Deep Beams", Journal of Advanced Concrete Technology, 2009.
Publication <1%

55 Ping Xiang, Akira Nishitani, Shohei Marutani, Kenzo Kodera, Tomohiko Hatada, Ryuta Katamura, Kiyoshi Kanekawa, Takashi Tanii. "Identification of yield drift deformations and evaluation of the degree of damage through <1%

the direct sensing of drift displacements", Earthquake Engineering & Structural Dynamics, 2016
Publication

56	M. Ghassemieh. "Seismic evaluation of reduced beam section frames considering connection flexibility : Seismic evaluation of reduced beam section frames", The Structural Design of Tall and Special Buildings, 01/2012 Publication	<1 %
57	Kaminosono, Takashi. "New RC Structural Elements", Series on Innovation in Structures and Construction, 2001. Publication	<1 %
58	Chien-Kuo Chiu, I-Hsiang Liao, Wen-Yu Jean. "Seismic design requirements for reinforced concrete piers considering aftershock-induced seismic hazard", Structure and Infrastructure Engineering, 2017 Publication	<1 %
59	Jinkoo Kim, Seeun An. "Optimal distribution of friction dampers for seismic retrofit of a reinforced concrete moment frame", Advances in Structural Engineering, 2016 Publication	<1 %
60	Jara, J.M.. "Seismic response of buildings with energy dissipating systems built in soft soils",	<1 %

Engineering Structures, 200905

Publication

61 Yasuhiro Hayashi. "Simulation analyses of buildings damaged in the 1995 Kobe, Japan, earthquake considering soil-structure interaction", Earthquake Engineering & Structural Dynamics, 04/1999 <1%

Publication

62 Wenjuan Lou. "Three-dimensional wind load effects and wind-induced dynamic responses of a tall building with X-shape", The Structural Design of Tall and Special Buildings, 2009 <1%

Publication

Exclude quotes	On	Exclude matches	Off
Exclude bibliography	On		